N-Glycans Mediate the Apical Sorting of a GPI-anchored, Raft-associated Protein in Madin-Darby Canine Kidney Cells

Jürgen H. Benting, Anton G. Rietveld, and Kai Simons

European Molecular Biology Laboratory (EMBL), Cell Biology and Biophysics Programme, D-69012 Heidelberg, Germany; and Max Planck Institute for Molecular Cell Biology and Genetics, D-01307 Dresden, Germany

Abstract. Glycosyl-phosphatidylinositol (GPI)-anchored proteins are preferentially transported to the apical cell surface of polarized Madin-Darby canine kidney (MDCK) cells. It has been assumed that the GPI anchor itself acts as an apical determinant by its interaction with sphingolipid-cholesterol rafts. We modified the rat growth hormone (rGH), an unglycosylated, unpolarized secreted protein, into a GPI-anchored protein and analyzed its surface delivery in polarized MDCK cells. The addition of a GPI anchor to rGH did not lead to an increase in apical delivery of the protein. However, addition of N-glycans to GPI-anchored rGH resulted in predominant apical delivery, suggesting that N-glycans act as apical sorting signals on GPI-anchored proteins as they do on transmembrane and secretory proteins. In contrast to the GPI-anchored rGH, a transmembrane form of rGH which was not raft-associated accumulated intracellularly. Addition of N-glycans to this chimeric protein prevented intracellular accumulation and led to apical delivery.

Key words: lipid rafts • N-glycans • GPI-anchored proteins • Madin-Darby canine kidney cells • sorting

A very heterogeneous subset of cellular surface proteins including several receptors, enzymes, and adhesion molecules is tethered to the outer leaflet of cellular membranes through a glycosyl-phosphatidylinositol (GPI)[1] anchor. It has been found that most endogenous and exogenous GPI-anchored proteins and GPI-anchored fusion proteins are delivered predominantly to the apical surface of polarized epithelial cells (Lisanti et al., 1988, 1989; Brown et al., 1989; Soole et al., 1995; Kenworthy and Edidin, 1998). During their transport to the apical cell surface GPI-anchored proteins were shown to become insoluble in the nonionic detergent Triton X-100 (TX-100) at the level of the Golgi complex (Brown and Rose, 1992). Analysis of the TX-100–insoluble material revealed that cholesterol, sphingomyelin, and glycosphingolipids are enriched in these so-called detergent-insoluble glycosphingolipid complexes (DIGs). Currently, cholesterol and (glyco)-sphingolipids are believed to be detergent-insoluble because they form liquid ordered (l_o) lipid domains in the plane of the bilayer (Ahmed et al., 1997), also called lipid rafts (Simons and Ikonen, 1997). Lipid rafts are characterized by a higher degree of acyl chain order (Brown and London, 1998; Rietveld and Simons, 1998) than the surrounding lipid bilayer which is in a liquid disordered (l_d) phase. The correlation between the apical delivery of the raft-forming (glyco)-sphingolipids (van Meer, 1989), the raft association of proteins, and their apical delivery has led to the formulation of the raft hypothesis, which proposes that rafts function as platforms for the apical sorting of raft-associated proteins (Simons and van Meer, 1988; Simons and Ikonen, 1997). Based on this concept, raft association mediated by the lipid anchor is believed to be a determinant for the apical delivery of GPI-anchored proteins.

However, the function of the GPI anchor as an apical targeting determinant has been questioned recently and it is possible that apical sorting information in the protein moiety accounts for the apical delivery of GPI-anchored proteins (Arreaza and Brown, 1995; Brown and London, 1998). Previous studies have shown that the protein part of GPI-anchored decay acceleration factor (DAF), placental alkaline phosphatase (PLAP), and Thy-1 are secreted apically when attachment of the GPI anchor has been abrogated (Brown et al., 1989; Lisanti et al., 1989; Powell et al., 1991). Thus, the sorting information in the protein moiety is sufficient for apical delivery. Considering what sorting

Address correspondence to Kai Simons, European Molecular Biology Laboratory (EMBL), Cell Biology and Biophysics Programme, Postfach 102209, Meyerhofstrasse 1, D-69012 Heidelberg, Germany. Tel.: 49-6221-387-334. Fax: 49-6221-387-512. E-mail: Simons@EMBL-Heidelberg.de

1. *Abbreviations used in this paper:* DAF, decay acceleration factor; DIG, detergent-insoluble glycosphingolipid complex; GPI, glycosyl-phosphatidylinositol; LDL-R, human low density lipoprotein receptor; PLAP, placental alkaline phosphatase; rGH, rat growth hormone; TMD, transmembrane domain; TX-100, Triton X-100.

Table I. Localization and Glycosylation of Several Natural and Artificial GPI-anchored Proteins

Protein	Localization	Glycosylation	Cell type	Reference
PLAP*	Api	N	MDCK	Brown et al., 1989
DAF*	Api	N/0	Caco-2/SK-CO15	Lisanti et al., 1989
Thy-1*	Api	N	MDCK	Powell et al., 1991
5′-Nucleotidase	Api	N	MDCK	Kenworthy and Edidin, 1998
hGH-DAF‡	Api	—	MDCK	Lisanti et al., 1989
gD1-DAF	Api	N	MDCK	Lisanti et al., 1989
	Bl		FRT	Zurzolo et al., 1993
EGE′-Thy1§	Api	Yes‖	MDCK/CaCo-2	Soole et al., 1995
GP-2	Api	N	MDCK II/G	Mays et al., 1995
GPI-N-CAM	Api	N	MDCK	Powell et al., 1991
Glypican	Bl	Heparan sulfate	MDCK	Mertens et al., 1996

*Protein moiety is secreted apically. ‡hGH is nonglycosylated but is secreted apically (65%) from polarized MDCK cells. §Endoglucanase 1 from *Clostridium thermocellum.* ‖Glycosylation not specified.
Api, apical; Bl, basolateral.

information could be contained in the ectodomains of GPI-anchored proteins, it is important to note that N-glycans on secretory (Scheiffele et al., 1995) and N- and/or O-glycans on membrane proteins act as apical targeting signals (Yeaman et al., 1997; Gut et al., 1998). Because most GPI-anchored proteins that have been studied so far are N-glycosylated (Table I), it is possible that N-glycans are involved in the apical delivery of GPI-anchored proteins. This possibility is supported by the finding that in a Con A–resistant MDCK cell line which has an unknown defect in glycosylation, some endogenous GPI-anchored proteins are distributed in an unpolarized fashion (Lisanti et al., 1990).

To analyze the sorting information contained in a GPI anchor and thereby also the consequence of raft association for polarized sorting we expressed the nonglycosylated rat growth hormone (rGH0) linked to the GPI anchor signal of DAF (rGH0-DAF) in MDCK cells. rGH0 is secreted 40% apically and 60% basolaterally from MDCK cells (Gottlieb et al., 1986; Scheiffele et al., 1995). Comparable ratios have been found for the secretion of the unglycosylated secretory protein lysozyme (Kondor-Koch et al., 1985). Thus, the well characterized unpolarized secretion of rGH0 makes it a suitable protein moiety for the analysis of the sorting information of a GPI anchor. Furthermore, we compared the surface delivery of rGH0-DAF to the sorting of rGH12-DAF, engineered to contain two N-glycans which act as apical targeting signals on the secretory form of rGH12 (Scheiffele et al., 1995), to analyze whether N-glycans can act as apical targeting signal on GPI-anchored proteins as well. In addition, we expressed rGH0 and rGH12 fused to the transmembrane domain of the human low density lipoprotein receptor followed by 12 amino acids of its cytoplasmic tail (rGH-LDL-R), but lacking the basolateral targeting signals of the human LDL-R (Matter et al., 1992). The LDL-R does not associate with lipid rafts (Harder et al., 1998). Therefore, the fusion proteins rGH0-LDL-R and rGH12-LDL-R allow us to compare the surface delivery of a non–raft-associated protein in the absence and presence of known sorting signals.

We show that the GPI-anchored protein rGH0-DAF is delivered in an unpolarized fashion to the cell surface and that upon N-glycosylation rGH12-DAF is transported apically in MDCK cells. The non–raft-associated protein rGH0-LDL-R is transported inefficiently to the cell surface and accumulates intracellularly. The intracellular accumulation of rGH0-LDL-R can be prevented by the addition of N-glycans to the protein that act as apical sorting signals on both GPI-anchored and transmembrane proteins.

Material and Methods

Cell Lines and Cell Culture

MDCK cells strain II were grown in MEM (GIBCO BRL) containing 10% FCS, supplemented with penicillin (100 U/ml), streptomycin (100 μg/ml), and 2 mM glutamine (GIBCO BRL). A MDCK cell line stably expressing human PLAP was obtained from D. Brown (State University of New York at Stony Brook, Stony Brook, NY) (Brown et al., 1989). MDCK cells were grown on Transwell polycarbonate filters (Costar Corp.) as described previously (Pimplikar et al., 1994) for 3.5 d.

Antibodies

A rabbit polyclonal anti-PLAP antibody was from Dako, a rabbit polyclonal antibody against rGH was purchased from Biogenesis, and a rabbit anti–caveolin-1 antibody was obtained from Santa Cruz Biotechnology. The rabbit anti-gp80 was described previously (Urban et al., 1987).

Preabsorbed secondary rhodamine-conjugated anti–rabbit and anti–mouse antibodies were from Dianova.

Recombinant Adenoviruses and Expression Constructs

The DNA construct pRc-CMV/rGH0-DAF (Friedrichson and Kurzchalia, 1998) coding for a GPI-anchored rGH0 was kindly provided by Dr. T. Kurzchalia (MDC, Berlin, Germany). The cDNA was cut with HinDIII and subcloned into pAdTrack-CMV linearized with HinDIII to yield pAdTrack-CMV/rGH0-DAF. The construct pBK-CMV/rGH12-DAF coding for a doubly N-glycosylated rGH-DAF (rGH12) fusion protein was generated by ligating the NH_2-terminal fragment of rGH12 as an EcoRI-Acc65I fragment from pRmHa-3/rGH12 and the COOH-terminal fragment from pRc-CMV/rGH0-DAF as a Acc65I-HinDIII fragment into the vector pBK-CMV digested with EcoRI and HinDIII. The fusion protein was cut out with SalI and NotI and cloned into pShuttle-CMV to generate pShuttle-CMV/rGH12-DAF. Recombination of the shuttle vectors with the adenoviral backbone plasmid pAdEasy-1 was done in the *Escherichia coli* strain BJ5183 to generate pAdEasy-GFP/rGH0-DAF and pAdEasy/rGH12-DAF. Transfections and virus production were done as described in He et al. (1998). The expression constructs pcDNA-3/rGH0-LDL-R and rGH12-LDL-R coding for rGH0 and rGH12 fused to the transmembrane domain (TMD) and a truncated cytosolic tail (CT12 deletion) of human LDL-R (Matter et al., 1992) were generated as follows. The cytosolic tail (CT12) of the human LDL-R was amplified by PCR using the oligonucleotides 5′ GTTGGCGCGCCAGGAAGTAGCGTGAGGGCTCTG 3′ and 5′ CGCTCTAGATTATCAGTTGATGCTGTTGATGTTC 3′ and a

cDNA coding for human LDL-R as a template introducing a 5′ BssHII and a 3′ XbaI cleavage site, respectively. The PCR product was cloned into pGEM-T, sequenced, and ligated as a BssHII-XbaI fragment with rGH0 (HinDIII-BssHII fragment from pRc-CMV/rGH0-DAF) or rGH12 (EcoRI-BssHII fragment from pBK-CMV/rGH12-DAF) into pcDNA-3.

Transfection and Viral Infections of MDCK Cells

MDCK II cells were transfected with the expression constructs pcDNA-3/rGH0-LDL-R and rGH12-LDL-R by electroporation. Stably transfected cells were selected by treatment with 0.5 mg/ml G-418 (GIBCO BRL) for 2 wk and expressing clones were identified by immunofluorescence microscopy.

Before viral infection, MDCK cells grown for 3 d on Transwell polycarbonate filters were washed once from the apical side with infection medium (MEM with 0.2% BSA, 10 mM Hepes, pH 7.3). Infection with recombinant adenoviruses was done from the apical side in a total volume of 125 μl of infection medium for 90 min. The cells were then washed once with medium, cultured for 18–20 h and subsequently used either for surface transport assays or immunofluorescence microscopy.

Immunofluorescence Microscopy

MDCK cells, either filter-grown or grown on coverslips, were washed once in PBS containing 0.9 mM $CaCl_2$ and 0.5 mM $MgCl_2$ (PBS^+) and fixed for 30 min in 4% paraformaldehyde, washed with PBS^+, and quenched for 15 min with 10 mM NH_4Cl in PBS containing 0.1% TX-100 to permeabilize cells. Subsequently, the cells were washed twice in PBS^+ with 0.2% BSA and incubated for 1 h at room temperature. Next, the cells were incubated for 45 min at 37°C with the anti-rGH antibody diluted 1:100 in PBS/0.2% BSA. Excess antibody was removed by four washes with PBS/0.2% BSA. Primary antibodies were detected with TRITC-conjugated secondary antibodies diluted 1:200 in PBS/0.2% BSA for 45 min at 37°C. Finally, the cells were washed five times for 5 min with PBS under vigorous shaking and mounted in 90% glycerol in PBS containing 4% pyrogallol as an antifading reagent. Confocal microscopy was done on a LSM 510 Zeiss confocal microscope.

Floatation of DIGs

Cells grown on a 3-cm dish or on a 12-mm Transwell filter were scraped thoroughly in PBS and pelleted. Detergent extractions were done on ice with prechilled solutions. Cells were resuspended in 100 μl 10 mM Tris-HCl, pH 7.4, 150 mM NaCl, 1 mM EDTA (TNE) with CLAP (chymostatin, leupeptin, antipain, and pepstatin A, 25 μg/ml each final), and then 1 vol of 2% TX-100 in the same buffer was added. After 30 min of incubation the lysate was adjusted to 40% Optiprep (Nycomed Pharma As), overlaid with 30% and 5% Optiprep, and spun for 4 h in a SW-60 rotor at 28,000 rpm at 4°C. The fractions were collected from the top, precipitated in 10% TCA, separated by SDS-PAGE, and the distribution of individual proteins in the gradient was detected by Western blotting.

Selective Biotinylation of Apical and Basolateral Cell Surface Proteins

Filter-grown MDCK cells, either stable cell lines or virus infected, were washed three times for 10 min with PBS^+ at 4°C. Cells were then biotinylated with 1 mg/ml sulfo-NHS-LC-biotin (Pierce) in PBS^+ from the apical or basolateral side for 30 min at 4°C with PBS^+ containing 1% BSA present on the other side of the filter. After three washes with PBS^+ and quenching with 10 mM glycine in PBS^+ the filters were cut out and cells were lysed in TNE containing CLAP, 1% TX-100, and 0.2% SDS and were sonicated in a waterbath sonicator for 10 min at room temperature.

Cell Surface Transport Assay

18–20 h after viral infection filter-grown MDCK II cells were labeled with [^{35}S]methionine (2.5 mCi/ml) in methionine-free medium for 15 min and chased in the presence of cycloheximide (10 μg/ml) and excess methionine for 0–40 min. Subsequently, the cells were cooled to 4°C and washed three times for 10 min with ice-cold PBS^+. Surface biotinylation was performed as described above. rGH-GPI was immunoprecipitated from the lysate with 2 μl of the anti-rGH antibody and PLAP with 3 μl of the anti-PLAP antibody and with 25 μl of protein A–Sepharose CL-4B (Pharmacia) overnight. Beads were washed twice in buffer A (10 mM Tris-HCl, pH 7.4, 150 mM NaCl, 1 mM EDTA, 0.1% TX-100), three times in buffer A with 500 mM NaCl, and once in 10 mM Tris-HCl, pH 7.4. Proteins were eluted from the beads by boiling the sample twice for 5 min in 150 μl 0.6% SDS in TNE and the supernatant (300 μl) was mixed with 600 μl TNE containing 1.5% TX-100. Biotinylated proteins were precipitated with 10 μl streptavidin-agarose for 4 h at 4°C. Finally, the beads were washed twice in buffer A containing 500 mM NaCl, once in 10 mM Tris-HCl, pH 7.4, and bound proteins were analyzed by SDS-PAGE and autoradiography. Gp80 was immunoprecipitated from the apical and basolateral medium with 1 μl of the anti-gp80 antibody.

Results

N-Glycans as Apical Sorting Signals on GPI-anchored rGH

The expression of GPI-anchored forms of wild-type and doubly glycosylated rGH (rGH0 and rGH12) allowed us to analyze the targeting information contained in the GPI anchor in the presence or absence of additional sorting information in the protein. We used recombinant adenoviruses to express rGH0-DAF and rGH12-DAF (Fig. 1) in MDCK cells. The steady-state distribution of the fusion proteins in filter-grown MDCK cells was analyzed by confocal immunofluorescence microscopy. As can be seen in Fig. 2, rGH0-DAF was detectable at both the apical (Fig. 2 A) and the basolateral (Fig. 2 B) surface. The N-glycosylated rGH12-DAF showed a predominant apical distribution (Fig. 2 C) and was hardly detectable on the basolateral side (Fig. 2 D). Both GPI-anchored proteins were almost exclusively detected at the cell surface, and the presence of a significant intracellular pool was not observed. We further analyzed the steady-state distribution of the proteins in filter-grown MDCK cells by selective biotinylation of the apical or basolateral cell surface 18 h after adenoviral infection. As can be seen in Fig. 3 A, rGH0-DAF can be detected as expected on a Western blot as a single band of 29 kD (Friedrichson and Kurzchalia, 1998), whereas the expression of rGH12-DAF results in two products of higher molecular weight representing the mono- and doubly glycosylated form of rGH, the produc-

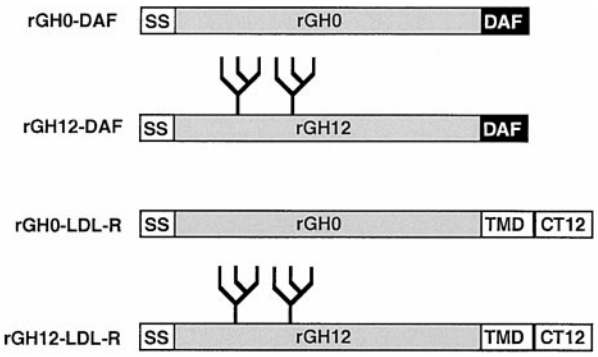

Figure 1. Schematic of fusion proteins used in this study. SS, signal sequence; rGH0, nonglycosylated rGH; rGH12, rGH with two artificial N-glycosylation sites represented by the trees; DAF, GPI anchor signal of decay acceleration factor; TMD, transmembrane domain of human LDL-R; CT12, truncated cytoplasmic tail of human LDL-R comprising 12 amino acids following the TMD lacking all basolateral sorting information.

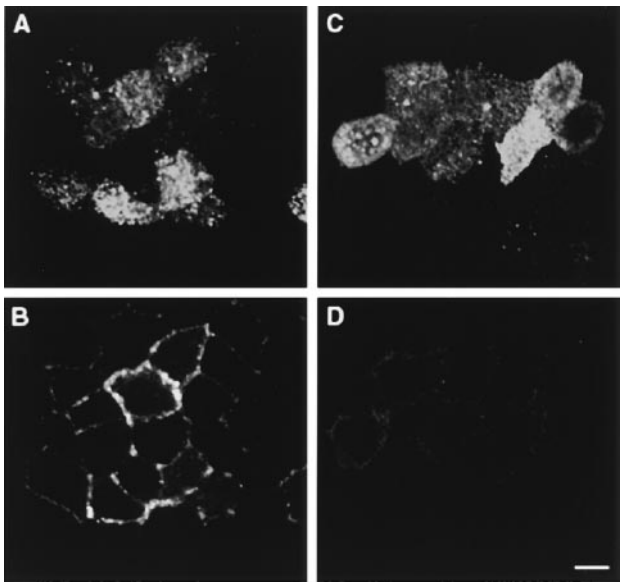

Figure 2. Localization of rGH0-DAF and rGH12-DAF in polarized MDCK cells. Polarized filter-grown MDCK cells were fixed 18 h after infection with adenovirus expressing rGH0-DAF (A and B) or rGH12-DAF (C and D). Cells were stained with the anti-rGH antibody and analyzed by confocal immunofluorescence microscopy. Apical optical sections (11 μm above the filter in A and C) and basolateral optical sections (5 μm above the filter in B and D) are shown. Note that rGH0-DAF localizes to the apical and the basolateral side of MDCK cells, whereas rGH12-DAF is predominantly found at the apical surface. Bar, 10 μm.

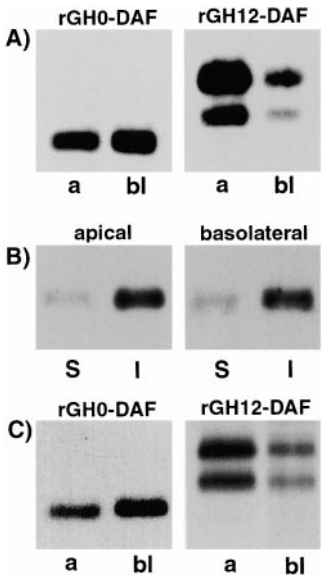

Figure 3. (A) Steady-state distribution of rGH0-DAF and rGH12-DAF. Adenovirus-infected filter-grown MDCK cells expressing rGH0-DAF or rGH12-DAF were surface-biotinylated from the apical (a) or basolateral (bl) surface. Biotinylated proteins were precipitated with streptavidin-agarose. The presence of precipitated rGH0-DAF and rGH12-DAF was analyzed on a Western blot. (B) Both the apical and the basolateral pools of rGH0-DAF are raft-associated. Polarized filter-grown MDCK cells were either biotinylated from the apical or basolateral side. The cells were extracted with TX-100 and DIGs were floated by Optiprep gradient centrifugation. The presence of rGH0-DAF in the soluble fraction (S, 40% Optiprep) and the insoluble floated material (I, 5–30% Optiprep interface) was analyzed on a Western blot. (C) Biosynthetic surface delivery of rGH0-DAF and rGH12-DAF. Filter-grown MDCK cells infected with adenovirus were pulse labeled with [^{35}S]methionine and chased for 40 min as described. Surface proteins were biotinylated from the apical (a) or basolateral (bl) side and rGH-DAF was immunoprecipitated. After elution from the protein A beads, the biotinylated fraction of rGH-DAF was precipitated with streptavidin-agarose and analyzed by SDS-PAGE and autoradiography.

tion of which has been described previously for the soluble rGH12 mutant (Scheiffele et al., 1995). By surface biotinylation, rGH0-DAF was detected at both the apical and basolateral surface in comparable quantities, whereas the N-glycosylated forms of rGH12-DAF were preferentially localized at the apical surface (Fig. 3 A).

We next analyzed the detergent insolubility of the apical and basolateral pools of the rGH0-DAF separately. Surface proteins of filter-grown cells were biotinylated from the apical or basolateral side and the cells were extracted with TX-100 on ice. The detergent-resistant fraction was floated in an Optiprep gradient centrifugation and analyzed for the presence of biotinylated rGH0-DAF (Fig. 3 B). Two fractions collected from the gradient are shown: the 5–30% Optiprep interface containing the DIGs (I), and the 40% Optiprep bottom fraction containing the solubilized material (S). We found that 90% of both the apical and the basolateral pool of the protein were floating to the 5–30% Optiprep interface, indicating that the large basolateral pool of rGH0-DAF was raft-associated also. The small basolateral pool of PLAP in MDCK cells has also reported to be resistant to TX-100 extraction (Arreaza and Brown, 1995). The raft association of newly synthesized PLAP has been shown to occur in the Golgi complex with a half-time between 20 and 40 min after synthesis (Brown and Rose, 1992). We found that rGH0-DAF acquires raft association with comparable kinetics as PLAP (data not shown) and assume that rGH0-DAF also becomes raft-associated at the level of the Golgi complex and is transported to both cell surfaces in rafts.

Next we analyzed the biosynthetic surface delivery of the proteins in pulse–chase experiments. Based on autoradiography, the nonglycosylated GPI-anchored rGH0-DAF was found to be delivered predominantly to the basolateral side of MDCK cells (Fig. 3 C). Quantification showed that after 40 min of chase only 40 ± 5% (n = 12) of rGH0-DAF was delivered to the apical surface and 60 ± 5% of the protein was delivered directly to the basolateral side (Fig. 4). In contrast, the mono- and doubly glycosylated forms of rGH12-DAF were both delivered 63 ± 5% (n = 12) to the apical surface (Fig. 3 C). Similar results were obtained in time course experiments at 20, 30, and 60 min of chase (data not shown). These results show that the sorting of GPI-anchored rGH0 is similar to that of secretory rGH0 in MDCK cells. The addition of N-glycans to GPI-anchored rGH-DAF clearly leads to increased apical delivery as it has been previously shown for the secretory form.

As a control we analyzed in parallel the apical delivery of PLAP in a stable MDCK cell line (Brown et al., 1989) and the polarized secretion of gp80 (Urban et al., 1987) in adenovirus-infected cells. Under our experimental conditions PLAP was delivered 82 ± 5% (n = 6) to the apical surface of MDCK cells (Fig. 4), as reported previously (Brown et al., 1989). Also, gp80 was secreted from adenovirus-infected cells predominantly into the apical medium (Fig. 4). Therefore, we conclude that the unpolarized surface delivery of rGH0-DAF does not result from a failure of the cells in polarized sorting. Moreover, identical

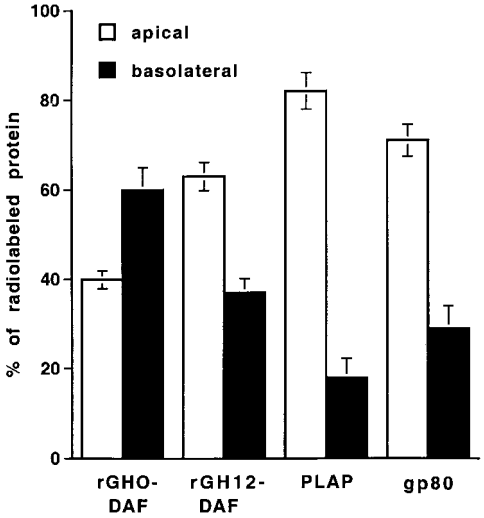

Figure 4. Quantification of biosynthetic surface delivery of rGH0-DAF, rGH12-DAF, PLAP, and gp80. The surface delivery of [^{35}S]methionine–labeled rGH0-DAF, rGH12-DAF, and PLAP was analyzed after a 40-min chase as described and quantified by PhosphoImaging. Apical and basolateral secretion of gp80 was analyzed by immunoprecipitation from the apical and basolateral medium of adenovirus-infected MDCK cells expressing rGH-DAF.

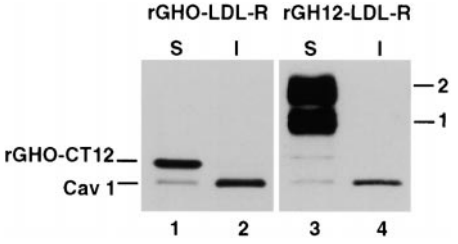

Figure 5. rGH-LDL-R fusion proteins are not raft-associated. TX-100 extraction and floatation of MDCK cell lines expressing rGH0-LDL-R (lanes 1 and 2) or rGH12-LDL-R (lanes 3 and 4). The presence of the fusion proteins and of caveolin-1 (Cav 1) in the soluble fraction (S, 40% Optiprep, lanes 1 and 3) and the insoluble floated material (I, 5–30% Optiprep interface, lanes 2 and 4) was analyzed by Western blot. The bands corresponding to monoglycosylated rGH-LDL-R and doubly glycosylated rGH-LDL-R are marked with 1 and 2, respectively (lanes 3 and 4).

results were obtained from a cell line stably expressing rGH0-DAF.

Our data demonstrate that the attachment of a GPI anchor to a protein is sufficient for raft association but not sufficient for predominant apical delivery. Furthermore, the experiments provide evidence that N-glycans can act as apical targeting signals on GPI-anchored proteins.

Reduced Cell Surface Transport of a Non–Raft-associated, Nonglycosylated Membrane Protein

To address the question of how a non–raft-associated, nonglycosylated protein is transported in MDCK cells, we constructed chimeric transmembrane proteins consisting of rGH0 or rGH12 as the ectodomain, and the TMD and the CT12 truncation of the cytoplasmic tail of the human LDL-R (Fig. 1). The CT12 mutation of the human LDL-R (Matter et al., 1992) comprises the first 12 amino acids of the cytoplasmic tail and lacks all basolateral sorting information. As a consequence, the LDL-R CT12 mutation is transported to the apical cell surface presumably due to the N- and O-glycans in its ectodomain. Thus, the chimeric rGH0-LDL-R can be considered as a non–raft-associated protein which lacks known sorting information in the ectodomain, the TMD, and the cytosolic tail. In parallel, we included the N-glycosylated rGH12-LDL-R fusion protein to analyze the role of N-glycans for the polarized sorting of membrane proteins. We generated stable MDCK cell lines expressing rGH0-LDL-R or rGH12-LDL-R. To confirm that the fusion proteins were not raft-associated, as predicted, the cell lines were extracted with TX-100 and the detergent-resistant membranes were floated in an Optiprep gradient centrifugation (Fig. 5). Fractions were collected from the gradient as described in Fig. 3 B. rGH0- and rGH12-LDL-R were detected exclusively in the bottom fraction containing the solubilized material (Fig. 5, lanes 1 and 3). As a marker protein for rafts we analyzed the distribution of caveolin-1 in this gradient. The majority of caveolin-1 is detectable in the DIG fraction (Fig. 5, lanes 2 and 4), showing that during extraction the non-raft membrane fusion proteins were efficiently solubilized whereas raft-associated proteins were not.

The distribution of the fusion proteins was analyzed by immunofluorescence microscopy in unpolarized MDCK cells. As can be seen in Fig. 6 A, rGH0-LDL-R was detected at steady state in the perinuclear region, resembling the Golgi complex, and to a lower extent at the plasma membrane. In contrast, the glycosylated rGH12-LDL-R shows a clear cell surface staining and only a minor fraction is visible in internal structures (Fig. 6 B).

The strong internal staining of rGH0-LDL-R (Fig. 6 A) prompted us to compare the amount of the protein present on the cell surface with the amount of protein that accumulated within the cells at steady state. Polarized filter-grown cells were surface-biotinylated simultaneously from the apical and basolateral sides. The biotinylated surface proteins were precipitated from the cell lysate with streptavidin-agarose. The unbound nonbiotinylated proteins in the depleted supernatant were precipitated with TCA. The presence of the fusion proteins was analyzed in both fractions on Western blots and quantified using NIH Image software. Only 30 ± 6% (n = 4) of the total rGH0-LDL-R were precipitated by streptavidin-agarose (Fig. 7 A, lane 1), whereas 70 ± 6% of the molecules were left in the supernatant (Fig. 7 A, lane 2) and therefore are considered as being accumulated within the cells. Thus, the nonglycosylated, non-raft membrane protein rGH0-LDL-R accumulated intracellularly and was transported inefficiently to the cell surface. In contrast, the majority of rGH12-LDL-R (82 ± 4%, n = 3) was biotinylated and precipitated by streptavidin-agarose. We did not find a significant difference between the efficiency of surface transport of mono- and doubly glycosylated rGH-LDL-R.

Finally, we analyzed the surface distribution of rGH12-LDL-R by confocal immunofluorescence microscopy in

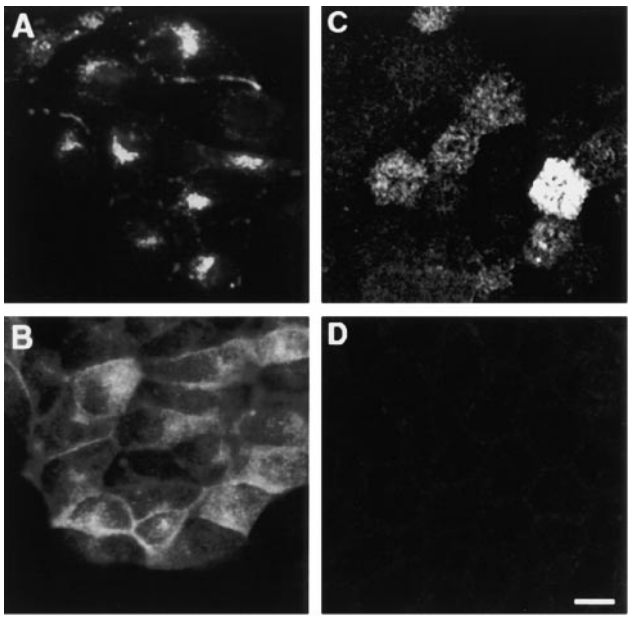

Figure 6. Localization of rGH0-LDL-R and rGH12-LDL-R in unpolarized MDCK cells by immunofluorescence microscopy (A and B). rGH0-LDL-R is detected mainly in internal perinuclear structures (A) whereas rGH12-LDL-R shows a clear surface staining (B). Confocal immunofluorescence microscopy on filter-grown MDCK cells expressing rGH12-LDL-R (C and D). An apical confocal section 11.5 μm above the filter (C) and a basolateral section (D, 6.5 μm above the filter) are shown. Note that rGH12-LDL-R was almost exclusively detected at the apical cell surface. Bar, 10 μm.

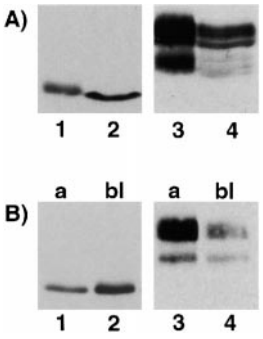

Figure 7. Intracellular accumulation of rGH0-LDL-R (A) and apical localization of rGH12-LDL-R at steady state (B). (A) The majority of rGH0-LDL-R accumulates intracellularly, whereas rGH12-LDL-R is mainly at the cell surface. Total surface biotinylation of filter-grown MDCK cell lines expressing rGH0-LDL-R (lanes 1 and 2) or rGH12-LDL-R (lanes 3 and 4). Biotinylated surface proteins were precipitated with streptavidin-agarose and are loaded in lanes 1 and 3. Nonbiotinylated (intracellular) proteins left in the supernatant after depletion of biotinylated proteins are shown in lanes 2 and 4. The presence of the rGH-fusion proteins in the fractions was analyzed on a Western blot. (B) Steady-state distribution of rGH0-LDL-R and rGH12-LDL-R. Surface biotinylation of filter-grown MDCK cell lines expressing rGH0-LDL-R (lanes 1 and 2) or rGH12-LDL-R (lanes 3 and 4) from the apical (a) or basolateral side (bl). Biotinylated proteins were precipitated with streptavidin-agarose. The presence of precipitated rGH0-LDL-R and rGH12-LDL-R was analyzed on a Western blot.

polarized MDCK cells and found that the glycosylated fusion protein was almost exclusively localized at the apical surface (Fig. 6 C), and only little basolateral staining was detectable (Fig. 6 D). The steady-state distribution of both fusion proteins was further analyzed by surface biotinylation of filter-grown cells. We found that the majority of the cell surface fraction of rGH0-LDL-R was at the basolateral cell surface (Fig. 7 B, lane 2), whereas the glycosylated rGH12-LDL-R was predominantly detected at the apical side (Fig. 7 B, lane 3). This shows that N-glycans can act as apical sorting signals on non-raft proteins.

Discussion

In this paper, we have analyzed whether association of proteins to lipid rafts by a GPI anchor leads to predominant apical delivery from the TGN in MDCK cells. Here, we show that when rGH0 is GPI-anchored the basolateral and the apical surface delivery is 60 and 40%, respectively. Previous studies in our lab showed that the secretory form of rGH0 is secreted 60% basolaterally and 40% apically in MDCK cells (Scheiffele et al., 1995). These data demonstrate that for rGH GPI anchoring is not sufficient for preferential apical delivery. Our results are in agreement with the finding that free GPI anchors are delivered unpolarized to the cell surface in MDCK cells (van't Hof et al., 1995). Preferential apical delivery of GPI-anchored rGH was obtained after addition of N-glycans to the protein, suggesting that N-glycans act as an apical sorting signal on GPI-anchored proteins. We assume that the presence of glycans on GPI-anchored proteins accounts for the predominant apical delivery in epithelial cells (Table I), as they do on secretory proteins, on rGH12-LDL-R, and on glycosylated transmembrane proteins which lack basolateral sorting signals (Yeaman et al., 1997; Gut et al., 1998).

Nevertheless, mechanisms different from glycan-mediated sorting may also lead to preferential apical delivery of secretory and GPI-anchored proteins. Lisanti and coworkers found that GPI-anchored nonglycosylated human growth hormone was apically localized in MDCK cells at steady state (Lisanti et al., 1989). However, also the nonglycosylated human GH was secreted in a polarized fashion, on average 65% apically (Lisanti et al., 1989), and we assume that the protein contains apical sorting information different from glycans. Interestingly, the heparan-sulfated GPI-anchored glypican is delivered predominantly to the basolateral surface of MDCK cells indicating that sulfated glycosaminoglycans act as basolateral sorting signals on GPI-anchored proteins (Mertens et al., 1996). This supports our finding that sorting signals on the protein influence the surface delivery of GPI-anchored proteins to the apical and basolateral cell surface of polarized cells.

Apical Delivery of Glycosylated Proteins

One interesting observation presented in this paper is the intracellular accumulation of the non–raft-associated rGH0-LDL-R which can be overcome by the addition of N-glycans. The same phenomenon was seen previously by Gut et al. (1998) who demonstrated that occludin lacking its basolateral determinants accumulated in the Golgi complex. Several other reports have suggested that mutant membrane proteins not being included in DIGs and lacking glycans are arrested intracellularly (Guan and Rose, 1984; Alonso et al., 1997; Gut et al., 1998). Addition of N-glycans to these proteins led to their delivery to the

(apical) cell surface (Guan et al., 1985; Gut et al., 1998), as we have found for rGH12-LDL-R. Moreover, the TX-100–soluble bovine enteropeptidase (Zheng et al., 1999) and many glycosylated basolateral proteins are sorted apically upon deletion of their cytoplasmic basolateral sorting signals (Rodriguez-Boulan and Powell, 1992; Matter and Mellman, 1994). To account for the predominant apical delivery of glycosylated secretory proteins, as well as raft and non–raft-associated membrane proteins, the existence of raft-associated lectins in the apical raft pathway was postulated (Fiedler et al., 1994; Simons and Ikonen, 1997). This hypothesis will remain speculative until such lectins have been identified to perform the postulated functions. A corollary of this hypothesis is that N-glycosylated proteins having basolateral sorting determinants would associate preferentially with the basolateral sorting machinery and therefore escape apical delivery mediated by association to raft lectins. These putative lectins would cluster glycosylated proteins lacking basolateral sorting signals as well as raft-associated glycoproteins. Thus, clusters of rafts would be formed on the luminal side of the Golgi complex which then bud out to form the apical transport containers. This raft clustering would be further facilitated by the apical transport machinery which links up with the putative lectin and potentially involves annexin XIIIb (Fiedler et al., 1995; Lafont et al., 1998), VIP21/caveolin-1 homo-oligomers (Scheiffele et al., 1998), and VIP17/MAL (Cheong et al., 1999). Previous investigations on apical cargo molecules have shown that diminishing drastically the levels of sphingolipids and cholesterol in MDCK cells leads to a decrease in the apical delivery of raft-associated proteins such as GPI-anchored proteins and influenza virus hemagglutinin but also of the N-glycosylated secretory protein gp80 (Mays et al., 1995; Keller and Simons, 1998). These reductions in cellular sphingolipid and cholesterol also decreased the association of these apical proteins with lipid rafts as measured by the DIG criterion, i.e., TX-100 insolubility and floatation to low density in gradient centrifugation (Scheiffele et al., 1997). In addition, depletion of only 25% of the cellular cholesterol led to intracellular accumulation of GPI-anchored proteins (Hannan and Edidin, 1996). These data strongly indicate that the apical pathway is dependent on rafts. Support for such a model for apical delivery comes from the finding that apically sorted GPI-anchored proteins, in this case gD1-DAF in MDCK cells, were found to be relatively immobile upon arrival at the apical cell surface, whereas GPI-anchored proteins missorted to the basolateral side dispersed more rapidly (Hannan et al., 1993).

Alternative models for the role of glycans in apical delivery have also been forwarded based on glycans affecting the folding of proteins and stabilizing a transport-permissive conformation (Rodriguez-Boulan and Gonzalez, 1999).

VIP36 was a candidate for a lectin involved in apical sorting (Fiedler and Simons, 1996). However, recent results from our lab have shown that VIP36 does not move beyond the Golgi complex and cycles in the early secretory pathway (Füllekrug et al., 1999). The existence of a raft-associated lectin in the apical pathway is purely conjectural. As already mentioned above, there are also several examples of proteins that are neither glycosylated nor associated with DIGs and these proteins are nevertheless delivered preferentially to the apical membrane (Alonso et al., 1997; Marzolo et al., 1997). These proteins could be linked by other proteins to the apical raft machinery or, alternatively, use an apical pathway not using sphingolipid-cholesterol rafts as sorting platforms.

How Are Lipid Rafts Transported Basolaterally?

We found that 60% of rGH0-DAF is delivered to the basolateral surface of MDCK cells. This shows that rafts are not restricted to the apical pathway. Clearly, the basolateral plasma membrane contains raft lipids, but in lower concentrations than in the apical membrane (Simons and van Meer, 1988), and raft-associated proteins. For example, mutant influenza virus hemagglutinin containing a tyrosine-based basolateral sorting signal in its cytoplasmic tail and CD44 are transported to the basolateral surface of MDCK cells and are raft-associated (Neame and Isacke, 1993; Naim et al., 1995; Neame et al., 1995). In addition, caveolae, invaginated raft domains containing caveolin-1/-2 hetero-oligomers (Scheiffele et al., 1998), are enriched on the basolateral cell surface of MDCK cells. Two recent insights into the behavior of rafts also have to be considered. First, lipid rafts are small, $<$70 nm in diameter, and thus below the resolution of the light microscope (Varma and Mayor, 1998), and second, cross-linking of raft components, e.g., by raft-associated lectins, is a dynamic process in which cross-linked and non–cross-linked raft-associated proteins can separate from each other. When raft proteins, e.g., a GPI-anchored protein, are patched with a cross-linking antibody on the surface of a fibroblast, a second non–cross-linked raft protein, e.g., influenza virus hemagglutinin, is predominantly excluded from the cross-linked patches (Harder et al., 1998). However, if the two proteins are both patched by simultaneous application of antibodies, they co-cluster. Therefore, we assume that nonglycosylated GPI-anchored rGH is mostly excluded from the clustered rafts that form the apical containers and is available for transport elsewhere. Possibly, rGH0-DAF could be delivered together with rafts containing proteins with basolateral sorting determinants to the basolateral plasma membrane.

One important conclusion is that raft-based sorting is not an all or none phenomenon, demonstrated in this paper by the fact that raft association via a GPI anchor is not sufficient for predominant apical delivery. Several layers of interactions with raft platforms can be envisaged that lead to efficient surface-specific delivery of rafts and their associated proteins.

We thank P. Keller for advice during the generation of recombinant adenoviruses, K. Ekroos for cell culture, and T. Kurzchalia and C. Koch-Brandt for the generous gift of cDNAs and antibodies. We thank Suzanne Eaton and Derek Toomre for critical reading of the manuscript. Many thanks to Iris Ansorge and Konrad for valuable discussions and support.

J. Benting and A. Rietveld were supported by an EMBO long-term fellowship. This work was supported by the Commission of the European Community and grant SFB 352.

Submitted: 11 May 1999
Revised: 8 June 1999
Accepted: 11 June 1999

References

Ahmed, S.N., D.A. Brown, and E. London. 1997. On the origin of sphingolipid-cholesterol rich detergent-insoluble domains in cell membranes: physiological concentrations of cholesterol and sphingolipid induce formation of a detergent-insoluble, liquid-ordered lipid phase in model membranes. *Biochemistry*. 36:10944–10953.

Alonso, M.A., L. Fan, and B. Alarcon. 1997. Multiple sorting signals determine apical localization of a non-glycosylated integral membrane protein. *J. Biol. Chem*. 272:30748–30752.

Arreaza, G., and D.A. Brown. 1995. Sorting and intracellular trafficking of a glycosylphosphatidylinositol-anchored protein and two hybrid transmembrane proteins with the same ectodomain in Madin-Darby canine kidney epithelial cells. *J. Biol. Chem*. 270:23641–23647.

Brown, D.A., and E. London. 1998. Functions of lipid rafts in biological membranes. *Annu. Rev. Cell Dev. Biol.* 14:111–136.

Brown, D.A., and J.K. Rose. 1992. Sorting of GPI-anchored proteins to glycolipid-enriched membrane subdomains during transport to the apical cell surface. *Cell.* 68:533–544.

Brown, D.A., B. Crise, and J.K. Rose. 1989. Mechanism of membrane anchoring affects polarized expression of two proteins in MDCK cells. *Science.* 245: 1499–1501.

Cheong, K.H., D. Zacchetti, E.E. Schneeberger, and K. Simons. 1999. VIP17/MAL, a lipid raft-associated protein is involved in apical transport in MDCK cells. *Proc. Natl. Acad. Sci. USA*. 96:6241–6248.

Fiedler, K., and K. Simons. 1996. Characterization of VIP36, an animal lectin homologous to leguminous lectins. *J. Cell Sci.* 109:271–276.

Fiedler, K., R.G. Parton, R. Kellner, T. Etzold, and K. Simons. 1994. VIP36, a novel component of glycolipid rafts and exocytic carrier vesicles in epithelial cells. *EMBO (Eur. Mol. Biol. Organ.) J.* 13:1729–1740.

Fiedler, K., F. Lafont, R.G. Parton, and K. Simons. 1995. Annexin XIIIb: a novel epithelial specific annexin is implicated in vesicular traffic to the apical plasma membrane. *J. Cell Biol.* 128:1043–1053.

Friedrichson, T., and T.V. Kurzchalia. 1998. Microdomains of GPI-anchored proteins in living cells revealed by crosslinking. *Nature.* 394:802–805.

Füllekrug, J., P. Scheiffele, and K. Simons. 1999. VIP36 localisation to the early secretory pathway. *J. Cell Sci.* In press.

Gottlieb, T.A., G. Beaudry, L. Rizzolo, A. Colman, M. Rindler, M. Adesnik, and D.D. Sabatini. 1986. Secretion of endogenous and exogenous proteins from polarized MDCK cell monolayers. *Proc. Natl. Acad. Sci. USA*. 83: 2100–2104.

Guan, J.-L., and J.K. Rose. 1984. Conversion of a secretory protein into a transmembrane protein results in its transport to the Golgi complex but not to the cell surface. *Cell.* 37:779–787.

Guan, J.L., C.E. Machamer, and J.K. Rose. 1985. Glycosylation allows cell-surface transport of an anchored secretory protein. *Cell.* 42:489–496.

Gut, A., F. Kappeler, N. Hyka, M.S. Balda, H.-P. Hauri, and K. Matter. 1998. Carbohydrate-mediated Golgi to cell surface transport and apical targeting of membrane proteins. *EMBO (Eur. Mol. Biol. Organ.) J.* 17:1919–1929.

Hannan, L.A., and M. Edidin. 1996. Traffic, polarity, and detergent solubility of a glycosylphosphatidylinositol-anchored protein after LDL deprivation of MDCK cells. *J. Cell Biol.* 133:1265–1276.

Hannan, L.A., M.P. Lisanti, E. Rodriguez-Boulan, and M. Edidin. 1993. Correctly sorted molecules of a GPI-anchored protein are clustered and immobile when they arrive at the apical surface of MDCK cells. *J. Cell Biol.* 120: 353–358.

Harder, T., P. Scheiffele, P. Verkade, and K. Simons. 1998. Lipid domain structure of the plasma membrane revealed by patching of membrane components. *J. Cell Biol.* 141:929–942.

He, T.-C., S. Zhou, L.T. da Costa, K.W. Kinzler, and B. Vogelstein. 1998. A simplified system for generating recombinant adenoviruses. *Proc. Natl. Acad. Sci. USA*. 95:2509–2514.

Keller, P., and K. Simons. 1998. Cholesterol is required for surface transport of influenza virus hemagglutinin. *J. Cell Biol.* 140:1357–1367.

Kenworthy, A.K., and M. Edidin. 1998. Distribution of a glycosylphosphatidylinositol-anchored protein at the apical surface of MDCK cells examined at a resolution of <100 A using imaging fluorescence resonance energy transfer (published erratum appeared in *J. Cell Biol.* 1998. 142:883). *J. Cell Biol.* 142: 69–84.

Kondor-Koch, C., R. Bravo, S.D. Fuller, D. Cutler, and H. Garoff. 1985. Exocytic pathways exists to both the apical and the basolateral cell surface of the polarized epithelial cell MDCK. *Cell.* 43:297–306.

Lafont, F., S. Lecat, P. Verkade, and K. Simons. 1998. Annexin XIIIb associates with lipid microdomains to function in apical delivery. *J. Cell Biol.* 142:1413–1427.

Lisanti, M.P., M. Sargiacomo, L. Graeve, A.R. Saltiel, and E. Rodriguez-Boulan. 1988. Polarized apical distribution of glycosyl-phosphatidylinositol-anchored proteins in a renal epithelial cell line. *Proc. Natl. Acad. Sci. USA*. 85:9557–9561.

Lisanti, M.P., I.W. Caras, M.A. Davitz, and E. Rodriguez-Boulan. 1989. A glycophospholipid membrane anchor acts as an apical targeting signal in polarized epithelial cells. *J. Cell Biol.* 109:2145–2156.

Lisanti, M.P., A. Le Bivic, A.R. Saltiel, and E. Rodriguez-Boulan. 1990. Preferred apical distribution of glycosyl-phosphatidylinositol (GPI) anchored proteins: a highly conserved feature of the polarized epithelial cell phenotype. *J. Membr. Biol.* 113:155–167.

Marzolo, M.P., P. Bull, and A. Gonzalez. 1997. Apical sorting of hepatitis B surface antigen (HBsAg) is independent of N-glycosylation and glycosylphosphatidylinositol-anchored protein segregation. *Proc. Natl. Acad. Sci. USA*. 94:1834–1839.

Matter, K., and I. Mellman. 1994. Mechanisms of cell polarity: sorting and transport in epithelial cells. *Curr. Opin. Cell Biol.* 6:545–554.

Matter, K., W. Hunzicker, and I. Mellman. 1992. Basolateral sorting of LDL receptor in MDCK cells: the cytoplasmic domain contains two tyrosine-dependent targeting determinants. *Cell.* 71:741–753.

Mays, R.W., K.A. Siemers, B.A. Fritz, A.W. Lowe, G. van Meer, and W.J. Nelson. 1995. Hierarchy of mechanisms involved in generating Na/K-ATPase polarity in MDCK epithelial cells. *J. Cell Biol.* 130:1105–1115.

Mertens, G., B. van der Schueren, H. van den Berghe, and G. David. 1996. Heparan sulfate expression in polarized epithelial cells: the apical sorting of glypican (GPI-anchored proteoglycan) is inversely related to its heparan sulfate content. *J. Cell Biol.* 132:487–497.

Naim, H.Y., D.T. Dodds, C.B. Brewer, and M.G. Roth. 1995. Apical and basolateral coated pits of MDCK cells differ in their rates of maturation into coated vesicles, but not in the ability to distinguish between mutant hemagglutinin proteins with different internalization signals. *J. Cell Biol.* 129:1241–1250.

Neame, S.J., and C.M. Isacke. 1993. The cytoplasmic tail of CD44 is required for basolateral localization in epithelial MDCK cells but does not mediate association with the detergent-insoluble cytoskeleton of fibroblasts. *J. Cell Biol.* 121:1299–1310.

Neame, S.J., C.R. Uff, H. Sheikh, S.C. Wheatly, and C.M. Isacke. 1995. CD44 exhibits a cell type dependent interaction with Triton X-100 insoluble, lipid-rich, plasma membrane domains. *J. Cell Sci.* 108:3127–3135.

Pimplikar, S.W., E. Ikonen, and K. Simons. 1994. Basolateral protein transport in streptolysin O-permeabilized MDCK cells. *J. Cell Biol.* 125:1025–1035.

Powell, S.K., M.P. Lisanti, and E. Rodriguez-Boulan. 1991. Thy-1 expresses two signals for apical localization in epithelial cells. *Am. J. Physiol.* 260:C715–C720.

Rietveld, A., and K. Simons. 1998. The differential miscibility of lipids as the basis for the formation of functional membrane rafts. *Biochim. Biophys. Acta.* 1376:467–479.

Rodriguez-Boulan, E., and A. Gonzalez. 1999. Apical sorting signals in epithelia. *Trends Cell Biol.* In press.

Rodriguez-Boulan, E., and S.K. Powell. 1992. Polarity of epithelial and neuronal cells. *Annu. Rev. Cell Biol.* 8:395–427.

Scheiffele, P., J. Peranen, and K. Simons. 1995. N-glycans as apical sorting signals in epithelial cells. *Nature.* 378:96–98.

Scheiffele, P., M.G. Roth, and K. Simons. 1997. Interaction of influenza virus haemagglutinin with sphingolipid-cholesterol membrane domains via its transmembrane domain. *EMBO (Eur. Mol. Biol. Organ.) J.* 16:5501–5508.

Scheiffele, P., P. Verkade, A.M. Fra, H. Virta, K. Simons, and E. Ikonen. 1998. Caveolin-1 and -2 in the exocytic pathway of MDCK cells. *J. Cell Biol.* 140: 795–806.

Simons, K., and E. Ikonen. 1997. Functional rafts in cell membranes. *Nature.* 387:569–572.

Simons, K., and G. van Meer. 1988. Lipid sorting in epithelial cells. *Biochemistry*. 27:6197–6202.

Soole, K.L., M.A. Jepson, G.P. Hazlewood, H.J. Gilbert, and B.H. Hirst. 1995. Epithelial sorting of a glycosylphosphatidylinositol-anchored bacterial protein expressed in polarized renal MDCK and intestinal Caco-2 cells. *J. Cell Sci.* 108:369–377.

Urban, J., K. Parczyk, A. Leutz, M. Kayne, and C. Kondor-Koch. 1987. Constitutive apical secretion of an 80-kD sulfated glycoprotein in the polarized epithelial Madin-Darby canine kidney cell line. *J. Cell Biol.* 105:2735–2743.

van Meer, G. 1989. Lipid traffic in animal cells. *Annu. Rev. Cell Biol.* 5:247–275.

van't Hof, W., B.E. Rodriguez, and A.K. Menon. 1995. Nonpolarized distribution of glycosylphosphatidylinositols in the plasma membrane of polarized Madin-Darby canine kidney cells. *J. Biol. Chem*. 270:24150–24155.

Varma, R., and S. Mayor. 1998. GPI-anchored proteins are organized in submicron domains at the cell surface. *Nature.* 394:798–801.

Yeaman, C., A.H. Le Gall, A.N. Baldwin, L. Monlauzeur, A. Le Bivic, and E. Rodriguez-Boulan. 1997. The O-glycosylated stalk domain is required for apical sorting of neurotrophin receptors in polarized MDCK cells. *J. Cell Biol.* 139:929–940.

Zheng, X., D. Lu, and J.E. Sadler. 1999. Apical sorting of bovine enteropeptidase does not involve detergent-resistant association with sphingolipid-cholesterol rafts. *J. Biol. Chem*. 274:1596–1605.

Zurzolo, C., M.P. Lisanti, I.W. Caras, L. Nitsch, and E. Rodriguez-Boulan. 1993. Glycosyl-phosphatidylinositol-anchored proteins are preferentially targeted to the basolateral surface in Fischer rat thyroid epithelial cells. *J. Cell Biol.* 121:1031–1039.